Near-Real Time Global Biomass Burning Emissions Product from Multiple Geostationary Satellites

X. Zhang[a,*], S. Kondragunta[b], J. Ram[c], C. Schmidt[d], H-C. Huang[e]

[a]ERT @ NOAA/NESDIS/STAR, Camp Springs, Maryland, USA - Xiaoyang.zhang@noaa.gov
[b]NOAA/NESDIS/STAR, Camp Springs, Maryland, USA - Shobha.Kondragunta@noaa.gov
[c]IMSG @NOAA/NESDIS/STAR, Camp Springs, Maryland, USA - Jessica.Ram@noaa.gov
[d]Cooperative Institute for Meteorological Satellite Studies, University of Wisconsin, Madison, USA -chris.schmidt@ssec.wisc.edu
[e]IMSG @NOAA/NCEP, Camp Springs, Maryland, USA - ho-chun.huang@noaa.gov

Abstract - Near-real time estimates of biomass burning emissions are important for air quality monitoring and forecasting. We present here the preliminary analysis of global biomass burning emission product (GBBEP) produced from geostationary-satellite-derived fire radiative power (FRP) in near-real time. Specifically, the FRP is retrieved at an interval of 15 to 30 minutes using WF_ABBA_V65 (Wildfire Automated Biomass Burning Algorithm) from multiple geostationary satellites. The missing FRP detections are simulated by combining the available instantaneous FRP observations within a day and the representative ecosystem-dependent climatologic diurnal pattern of half-hourly FRPs. Finally, the diurnal variation in FRP is applied to quantify global emissions of PM2.5 (particulate mass for particles with diameter < 2.5 µm) and trace gases with a one-day latency. The algorithm is tested by analyzing global patterns in hourly biomass burning emissions for 2010.

Key words: Geostationary satellite, wildfire, biomass burning emissions, fire radiative power, diurnal pattern

1. INTRODUCTION

Biomass burning contributes to deteriorated air quality and impacts carbon cycle because of the large amount of aerosols and trace gases released into the atmosphere. A large number of research efforts are underway to derive biomass burning emissions on regional to global scales, mostly using satellite measurements (e.g., van der Werf, 2006, Wiedinmyer et al., 2006; Zhang et al., 2008). However, the quality of emission estimates is difficult to determine and the data derived from different methods vary substantially. This is due to the fact that the parameters (burned area, fuel loading, factor of combustion, and factor of emission) used for the estimates of biomass burning emissions are hard to quantify accurately. For example, burned areas derived from field inventory, satellite-based burn scars, and satellite hotspots differ by a factor of seven in North America and by two orders of magnitude across the globe (Boschetti et al., 2004). The uncertainty of emission factors is about 20-30% (Andreae and Merlet, 2001). The fuel loading from different datasets differs by more than 35% (Zhang et al., 2008).

Using fire radiative energy (FRE) to determine emissions has recently emerged as an alternative approach to estimate biomass burning emissions. Theoretically, satellites observe fires through the radiant component of the total energy released from fires. The FRE reflects a combination of the fire strength and size and is related to the rate of biomass consumption. Thus, it provides a means to directly measure biomass combustion (Wooster et al., 2003). FRE can be measured from satellites, which provide the instantaneous measurement of fire radiance representing the rate of FRE release (Kaufman et al., 1998; Wooster et al., 2003, Ichoku et al., 2008). The instantaneous FRE is defined as fire radiative power (FRP, Wooster et al., 2003). It is a proxy for the rate of consumption of biomass, which is a function of area being burned, fuel loading, and combustion efficiency.

We present here the preliminary results of global biomass burning emissions product (GBBEP) produced from multiple satellite-derived fire radiative power (FRP) in near-real time. The FRP is retrieved using WF_ABBA (Wildfire Automated Biomass Burning Algorithm) from a network of geostationary satellites consisting of two Geostationary Operation Environmental Satellites (GOES) which are operated by the National Oceanic and Atmospheric Administration (NOAA), the Meteosat Second Generation Satellites (Metosat-09) operated by the European Organization for the Exploitation of Meteorological Satellites (EUMETSAT), and the Multi-functional Transport Satellite (MTSAT) operated by the Japan Meteorological Agency (JMA). The GBBEP results are assessed using emission estimates from MODIS (Moderate Resolution Imaging Spectroradiometer) fire counts.

2. METHODOLOGY

2.1 Modeling Biomass Burning Emissions

Biomass burning emissions are generally modeled using four fundamental parameters. These parameters are burned area, fuel loading (biomass density), the fraction of combustion, and the factors of emissions for trace gases and aerosols. By integrating these parameters, biomass burning emissions can be estimated (Seiler and Crutzen, 1980):

$$E = ABCF \quad (1)$$

In equation (1), E represents the emissions from biomass burning (kg); A is the burned area (km^2); B is the biomass density (kg/km^2); C is the fraction of biomass consumed during a fire event; and F is the factor of the consumed biomass released as trace gases and smoke particulates. This simple model has been widely applied to estimate the emissions in regional and global scales (Ito and Penner, 2004; Reid et al., 2004; Wiedinmyer et al., 2006; Zhang et al., 2008). The accuracy of the emissions depends on the accuracy of fuel loadings and burned areas which have large uncertainties (Zhang et al., 2008).

*Corresponding author.

Alternatively, Wooster (2002) demonstrated a linear relationship between fuel consumption and total emitted fire radiative energy. This is due to the fact that the total amount of energy released per unit mass of dry fuel fully burned is consistent across vegetation types and fuel types. Thus, Wooster (2002) derived an algorithm to estimate biomass burning emission using the formula:

$$E = FRE \times \beta \times F = \int_{t1}^{t2} FRP dt \times \beta \times F \qquad (2)$$

In equation (2), t_1 and t_2 are the beginning and ending time of a fire event, β is biomass combustion rate, and F is the emission factor.

The biomass combustion rate (β) is assumed to be a constant. The laboratory-controlled experiments in a combustion chamber demonstrate that the rate of dry fuels combusted per FRP unit ranges from 0.24-0.78 kg/MJ but the overall regression rate is 0.453 kg/MJ (Freeborn et al, 2008). However, the biomass combustion rate is 0.368±0.015 kg/MJ based on field controlled experiments regardless of the land-surface conditions (Wooster et al., 2005). This relationship has been applied directly to measure the amount of biomass combusted by integrating SEVIRI FRP observations over time across a regional scale (Roberts et al. 2005). Thus, this approach is also adopted in our study.

An emission factor (F) is a representative value that is used to relate the quantity of a trace gas or aerosol species released into the atmosphere with a wildfire activity. The value is a function of fuel type and is expressed as the number of kilograms of particulate per ton (or metric ton) of the material or fuel. This study assigns the emission factor for each emitted species (CO2, CO, CH4, NOx, NH3, SO2, VOC, PM10, and PM2.5) with land cover type according to values published in literature (e.g., Andreae and Merlet, 2001; Wiedinmyer et al., 2006). The land cover type is stratified to forest, savanna, shrub, grass, and crop in this study and the corresponding emission factor is aggregated from values in literature.

2.2. Fire Radiative Power (FRP) from Geostationary Fire Product

Fire radiative power is operationally produced from geostationary satellites at NOAA using WF_ABBA algorithm (Prins et al., 1998; Weaver et al., 2004). Particularly, the WF_ABBA V65 detects instantaneous fires in sub-pixels using 3.9 and 10.7 μm infrared bands from a network of geostationary satellites (Table A). It then derives instantaneous fire radiative power from single middle infrared waveband based on algorithm developed by Wooster et al. (2005). This fire product contains the time of fire detection, fire location in latitude and longitude, instantaneous estimate of FRP, ecosystem type, and a quality flag (ranging from 0 to 5: flag 0 — subpixel instantaneous estimation of fire size and temperature, flag 1 — saturated fire pixel, flag 2 — cloud-contaminated fire pixel, flag 3 — high probability fire pixel, flag 4 — medium probability fire pixel, flag 5 — low probability fire pixel). Further, to minimize false fire detections, the WF_ABBA uses a temporal filter to exclude the fire pixels that are only detected once within the past 12 h (Schmidt and Prins, 2003).

Table A. Geostationary satellites and FRP detections from WF_ABBA V65.

Satellite/Sensor	Spatial coverage	Spatial Resolution (Nadir)	Observation frequency
GOES-11 and -13 Imager	North America and South America	4 km	30 min
Metosat-9 SEVIRI	Africa and Europe	3 km	15 min
MTSAT Imager	Asia and Australia	4km	30 min

The diurnal variation in FRP data is reconstructed using FRP climatologic diurnal pattern for each individual fire pixel. Because of the impacts of factors including extreme solar zenith angles, fire saturation, smoke, sensor noises, weak fires, and clouds, there are only about 40% of the instantaneous fire observations with good quality (Zhang and Kondraguntra, 2008). As a result, a large number of FRP values are poorly estimated or uncalculated. These values are simulated using a climatologic diurnal pattern in FRP based on the following steps. (1) The FRP values with good quality (flag 0) from 2002-2005 in North America are averaged in every half hour for forests, savannas, shrubs, grasses, and croplands, separately, when the observation time is converted from UTC to solar local time, (2) these half hourly FRP data are fitted using Fourier models to produce climatology of FRP diurnal pattern, (3) for an individual fire pixel, the diurnal FRP is generated by shifting the climatologic FRP curve in the given ecosystem. The offset of shift is determined using a least square method from the detected FRP (flag 0) for the given fire pixel and the corresponding values in the climatologic curve. This curve is directly used if the number of the detected FRP within a day is less than 3 for the fire pixel, (4) the fire in a pixel is assumed to be continuous between first and last instantaneous observations (flags 0-5) if the gap is less than four hours, (5) the fire in a pixel is assumed to extend two hours prior and post instantaneous fire detections, (6) total FRE for the given pixel is the integration of the FRP during the fire period.

In near real time monitoring, WF_ABBA V65 fire products are automatically downloaded from NOAA ftp sites (ftp://140.90.213.161/FIRE/forPo/). The diurnal pattern of FRP is then generated based on fire observations during 24 hours in previous day globally. As a result, the global biomass burning emissions are produced with a latency of one to two days across the globe.

2.3 Assessment of the Estimates of Biomass Burning Emissions in GBBEP

We compare our GBBEP black and organic carbon values with those from Quick Fire Emission Dataset Version 1 (QFED v1, http://geos5.org/wiki/index.php?title=Quick_Fire_Emission_Dataset_%28QFED%29). The latter is derived using MODIS fire count products from both Aqua and Terra satellites and constant emission factors that are calibrated against Global Fire Emissions Data (GFED, van der Werf et al., 2006). Such comparison could produces the uncertainty of different products.

3. RESULTS

We estimate various trace gases and aerosol released from wildfires, but only PM2.5 emissions are illustrated in the following because all emission species show a similar pattern. Figure 1 presents the spatial pattern of the cumulated PM2.5 emissions from wildfires between DOY (day of year) 56 and 365 in 2010. The PM2.5 values are large in South America and Africa while the values are relatively small in Europe and Asia. In most of the southern Brazil and Bolivia in South America, the PM2.5 emission values are generally larger than $1.0x10^6$ kg in a geographical grid of 0.333°, where the largest emissions could be more than $5.0x10^6$ kg. Similarly, large emission in Africa occurs in Zaire, Angola, and southern Sudan. However, emissions are not estimated for the regions of India and most of Russia and Siberia because of the lack of coverage from geostationary satellites.

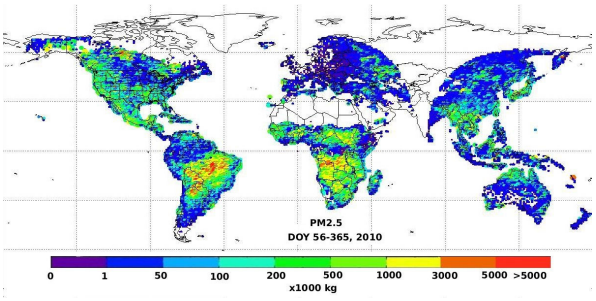

Figure 1. Estimates of global biomass burning emissions in a geographical grid of 0.333° between February 25 and December 31, 2010.

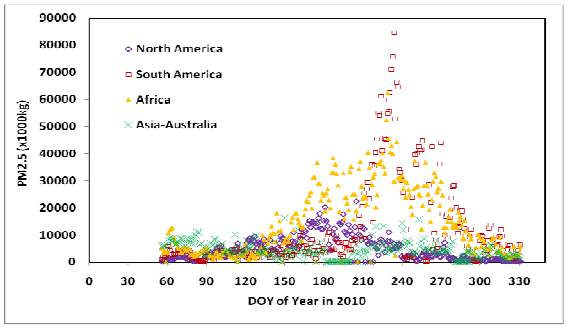

Figure 2. Daily PM2.5 emissions estimated from multiple geostationary satellites in 2010.

Figure 2 presents daily emission in various regions. Seasonal emissions in South America increases rapidly from late July, reaches peak in late August with a daily value as large as $8.46x10^7$ kg, and becomes limited in late October. In Africa, the emission season is long, which ranges from late May to late October with a daily emission value varying from about $3.0x10^7$ kg to $6.23x10^7$ kg. In North America, it ranges from May to September with a peak occurring in late July. The daily peak emission value is $2.23x10^7$ kg. In contrast, the seasonality of fire emissions in Asia and Australia is not distinguishable and the daily emission is generally less than $1.6x10^7$ kg.

Diurnal pattern in biomass burning emissions is strongly distinguishable in various continents (Figure 3). The PM2.5 emissions are mainly released from fires during 8:00–18:00 local solar time (LST) accounting to 80% of daily emissions. In Africa, the diurnal pattern exhibits a normal distribution. The peak occurs around 13:00 with a proportional value of 15%. Similar diurnal pattern appears in North America with a peak value of 11%. In contrast, the hourly emissions show a hat shape with a peak value about 11% in South America and Asia /Australia, respectively. The large hourly emissions occur earlier in Asia/Australia while it does later in South America.

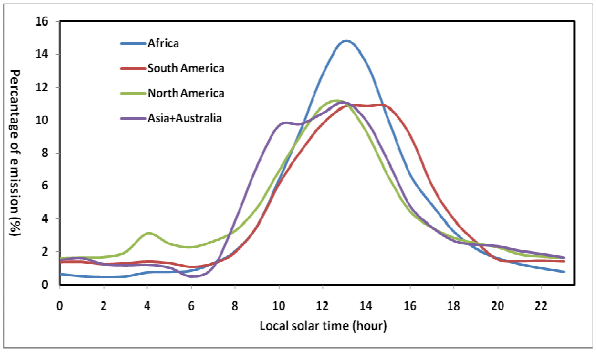

Figure 3. Diurnal variability in the PM2.5 emissions derived from multiple geostationary satellites.

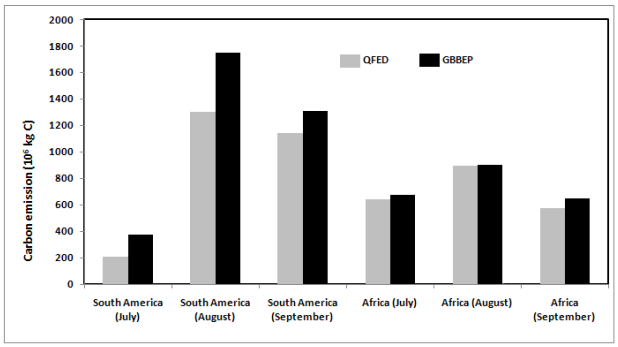

Figure 4. Comparison of monthly black and organic carbon estimated from GBBEP and QFED in Afica and South America, respectively.

The emission estimates from geostationary satellites are evaluated by comparing black and organic carbon emissions with QFED in Africa and South America (Figure 4). In Africa (around 25°S-5°N), the monthly emission value is similar in both data sets although GBBEP emissions are about 5%, 1%, and 13% larger than QFED emissins in July, August, and September, respectively. In contrast, the monthly QFED emssion in South America (around 35°S-10°N) is about 54%, 75%, and 87% of GBBEP value in July, August, and Sepetember, respectively. Overall, their values during these three months are compariable with a ratio (GBBEP/QFED) of 1.3 and 1.1 in South America and Africa. The large difference in South America (particularly in July and August) is likely associated with the fact that fire detections from both GOES-12 and GOES 13 are included in emission estimates. The GOES-

12 has better viewing geometry and scans South America more frequently, so that more fires are detected. Note that only GOES 13 is uaed to detect fires operationally in South America after August 2011.

4. CONCLUSIONS

Fire radiative power estimated from multiple geostationary satellites provides an opportunity to calculate global biomass burning emissions in near real time on hourly time scale, which will significantly contribute to aerosols and air quality modeling efforts. The estimate of biomass burning emissions from FRP avoids using the complex parameter of fuel loading and burned area. Thus it is a robust approach for the global estimates of biomass burning emissions. High frequent fire observations from geostationary satellites allow us to reconstruct diurnal pattern in FRP for a given fire pixel. This increases the number of observations that otherwise would be not reported due to cloud/smoke cover.

The biomass burning emissions estimated from multiple geostationary satellites are similar to the MODIS-fire-based estimates (QFED). This shows the feasibility of GBBEP algorithm although further validation is needed. Further, it should be noted that GBBEP provides limited coverage in high latitudes and no coverage in most regions across India and parts of Russia. .

REFERENCES

Andreae, M. O. and P. Merlet, "Emission of trace gasses and aerosols from biomass burning," Global Biogeochemical Cycles, 15(4), p.p. 955−966, 2001.

Boschetti, L., H. D. Eva, P. A. Brivio, and J. M. Grégoire, "Lessons to be learned from the comparison of three satellite-derived biomass burning products," Geophysical Research Letters, 31(L21501), doi:10.1029/2004GL021229, 2004.

Freeborn, P. H., M. J. Wooster, W. M. Hao, C. A. Ryan, B. L. Nordgren, S. P. Baker, and C. Ichoku, "Relationships between energy release, fuel mass loss, and trace gas and aerosol emissions during laboratory biomass fires," Journal of Geophysical Research-Atmospheres, 113, doi:10.1029/2007JD008679 ,2008.

Ichoku, C., and Y. J. Kaufman, "A method to derive smoke emission rates from MODIS fire radiative energy measurements," IEEE Transactions on Geoscience and Remote Sensing, 43(11), p.p. 2636-2649, 2005.

Ichoku, C., L. Giglio, M. J. Wooster, and L. A. Remer, "Global characterization of biomass-burning patterns using satellite measurements of fire radiative energy," Remote sensing of Environment, 112, p.p. 2950-2962, 2008.

Ito, A. and J. E. Penner, "Global estimates of biomass burning emissions based on satellite imagery for the year 2000," Journal of Geophysical Research, 109(D14S05), doi:10.1029/2003JD004423, 2004.

Kaufman, Y. J., C. O. Justice, L. P. Flynn, J. D. Kendall, E. M. Prins, L. Giglio, D. E. Ward, W. P. Menzel, and A. W. Setzer, "Potential global fire monitoring from EOS-MODIS," J. Geophys. Res., 103(D24), p.p. 32,215– 32,238, 1998.

Prins, E. M., J. M. Feltz, W. P. Menzel, and D. E. Ward, "An overview of GOES-8 diurnal fire and smoke results for SCAR-B and 1995 fire season in South America," Journal of Geophysical Research, 103(D24), p.p. 31821−31835, 1998.

Reid, J. S., E. M. Prins, D. L. Westphal, C. C. Schmidt, K. A. Richardson, S. A. Christopher, et al., "Real-time monitoring of South American smoke particle emissions and transport using a coupled remote sensing/box-model approach," Geophysical Research Letter, 31(L06107), doi:10.1029/2003GL018845, 2004.

Roberts, G., M. J. Wooster, G.L.W. Perry, N. Drake, L.M. Rebelo, F. Dipotso, "Retrieval of biomass combustion rates and totals from fire radiative power observations: application to southern Africa using geostationary SEVIRI imagery," Journal of Geophysical Research 110, D21111,, doi:10.1029/2005JD006018, 2005.

Seiler, W., P.J. Crutzen, "Estimates of gross and net fluxes of carbon between the biosphere and the atmosphere from biomass burning," Climatic Change, 2, p.p. 207–247, 1980.

van der Werf, G.R., J.T. Randerson, L. Giglio, G.J. Collatz, and P.S. Kasibhatla, "Interannual variability in global biomass burning emissions from 1997 to 2004," ACP, 6(11), p.p. 3423-3441, 2006.

Weaver, J. F., D. Lindsey, D. Bikos, C. C. Schmidt, and E. Prins, "Fire detection using GOES rapid scan imagery," Weather and Forecasting, 19, p.p. 496−510, 2004.

Wiedinmyer, C., B. Quayle, C. Geron, A. Belote, D. McKenzie, X. Zhang, S. O'Neill, K.K. Wynne, "Estimating emissions from fires in North America for air quality modeling," Atmospheric Environment, 40, p.p.3419–3432, 2006.

Wooster, M. J., "Small-scale experimental testing of fire radiative energy for quantifying mass combusted in natural vegetation fires," Geophys. Res. Lett., 29(21), 2027, doi:10.1029/2002GL015487, 2002.

Wooster, M. J., B. Zhukov, and D. Oertel, "Fire radiative energy for quantitative study of biomass burning: Derivation from the BIRD experimental satellite and comparison to MODIS fire products," Remote Sens. Environ., 86(1), p.p. 83–107, 2003.

Wooster, M. J., G. Roberts, G. L. W. Perry, and Y. J. Kaufman, "Retrieval of biomass combustion rates and totals from fire radiative power observations: FRP derivation and calibration relationships between biomass consumption and fire radiative energy release," J. Geophys. Res., 110, D24311, doi:10.1029/2005JD006318, 2005.

Zhang, X.Y., S. Kondragunta, C. Schmidt, and F. Kogan, "Near Real Time Monitoring of Biomass Burning Particulate Emissions (PM2.5) across Contiguous United States Using Multiple Satellite Instruments," Atmospheric Environment, 42, p.p. 6959-6972, 2008.

Zhang, X.Y., S. Kondragunta, **"**Temporal and spatial variability in biomass burned areas across the USA derived from the GOES fire product," Remote Sensing of Environment, 112, doi:10.1016/j.rse.2008.02.006, 2008.

ACKNOWLEDGMENTS

The views, opinions, and findings contained in those works are these of the author(s) and should not be interpreted as an official NOAA or US Government position, policy, or decision.